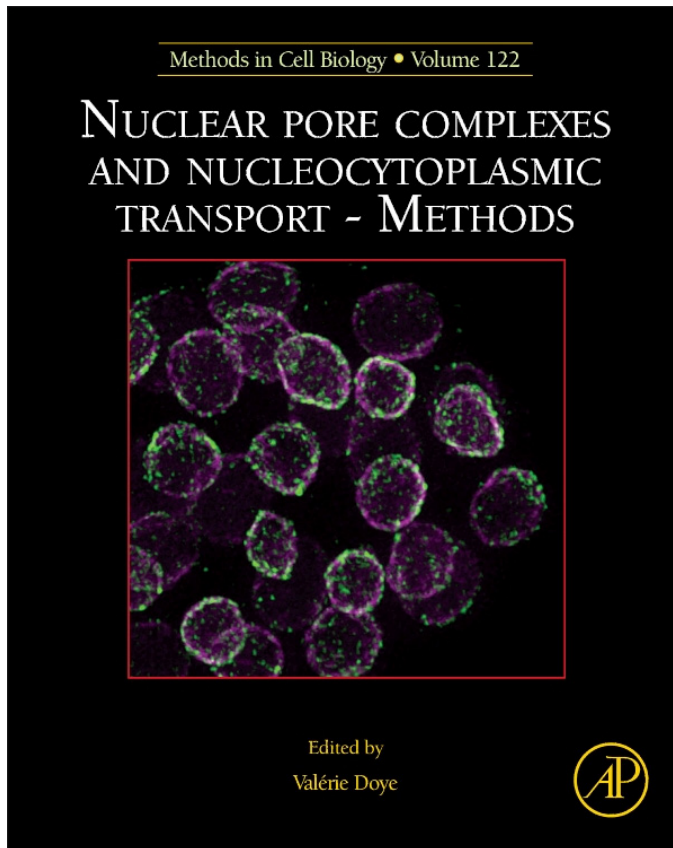


**Provided for non-commercial research and educational use only.  
Not for reproduction, distribution or commercial use.**

This chapter was originally published in the Book *Methods in Cell Biology*, Vol. 122 published by Elsevier, and the attached copy is provided by Elsevier for the author's benefit and for the benefit of the author's institution, for non-commercial research and educational use including without limitation use in instruction at your institution, sending it to specific colleagues who know you, and providing a copy to your institution's administrator.



All other uses, reproduction and distribution, including without limitation commercial reprints, selling or licensing copies or access, or posting on open internet sites, your personal or institution's website or repository, are prohibited. For exceptions, permission may be sought for such use through Elsevier's permissions site at:

<http://www.elsevier.com/locate/permissionusematerial>

From Peter Askjaer, Vincent Galy, and Peter Meister. Modern Tools to Study Nuclear Pore Complexes and Nucleocytoplasmic Transport in *Caenorhabditis elegans*. In Valérie Doye, editor: *Methods in Cell Biology*, Vol. 122, Burlington: Academic Press, 2014, pp.277-310.

ISBN: 978-0-12-417160-2

© Copyright 2014 Elsevier Inc.

Academic Press

# Modern Tools to Study Nuclear Pore Complexes and Nucleocytoplasmic Transport in *Caenorhabditis elegans*

# 13

**Peter Askjaer\***, **Vincent Galy<sup>‡,§</sup>**, and **Peter Meister<sup>¶</sup>**

\*Andalusian Center for Developmental Biology (CABD), CSIC/Junta de Andalucía/Universidad Pablo de Olavide, Carretera de Utrera, Seville, Spain

<sup>‡</sup>Sorbonne Universités, UPMC, Univ Paris 06, UMR7622, IBPS, F-75005 Paris, France

<sup>§</sup>CNRS, UMR7622, IBPS, F-75005 Paris, France

<sup>¶</sup>Cell fate and Nuclear Organization, Institute of Cell Biology, University of Bern, Baltzerstrasse 4, Bern, Switzerland

## CHAPTER OUTLINE

<b>Introduction</b> .....	<b>278</b>
<b>13.1 Forward and Reverse Genetics</b> .....	<b>279</b>
13.1.1 RNAi .....	285
13.1.2 Construction of RNAi Clone .....	286
13.1.3 Preparation of RNAi Plates .....	286
13.1.4 <i>C. elegans</i> RNAi Feeding .....	286
13.1.5 Materials .....	287
<b>13.2 Transgenesis</b> .....	<b>287</b>
<b>13.3 Live Imaging of Embryos</b> .....	<b>290</b>
13.3.1 Sample Preparation .....	295
13.3.2 How to Limit Phototoxicity .....	295
13.3.3 Materials .....	296
<b>13.4 In Vivo Methods to Evaluate Structural and Functional Integrity of the NE</b> .....	<b>296</b>
13.4.1 Preparation of Fluorescently Labeled Dextran for Germline Injection .....	298
<b>13.5 Immunofluorescence and Electron Microscopy</b> .....	<b>298</b>
13.5.1 Immunofluorescence .....	299
13.5.2 Transmission Electron Microscopy .....	302
<b>13.6 Interaction of Nups with Chromatin</b> .....	<b>303</b>

Summary and Future Perspectives.....	304
Acknowledgments .....	304
References .....	305

## Abstract

The nematode *Caenorhabditis elegans* is characterized by many features that make it highly attractive to study nuclear pore complexes (NPCs) and nucleocytoplasmic transport. NPC composition and structure are highly conserved in nematodes and being amenable to a variety of genetic manipulations, key aspects of nuclear envelope dynamics can be observed in great details during breakdown, reassembly, and interphase. In this chapter, we provide an overview of some of the most relevant modern techniques that allow researchers unfamiliar with *C. elegans* to embark on studies of nucleoporins in an intact organism through its development from zygote to aging adult. We focus on methods relevant to generate loss-of-function phenotypes and their analysis by advanced microscopy. Extensive references to available reagents, such as mutants, transgenic strains, and antibodies are equally useful to scientists with or without prior *C. elegans* or nucleoporin experience.

## INTRODUCTION

About half a century ago, Sydney Brenner decided to use *Caenorhabditis elegans*, a little (~1 mm) free-living soil nematode, to identify genes responsible for animal behavior and morphology (Brenner, 1974). *C. elegans* became immediately a popular model organism as transparency allowed observing organ development and muscle activity in the intact organism with noninvasive techniques. Careful observations by Sulston and colleagues uncovered that the cell lineage of *C. elegans* is invariant, implying that all individuals contain a fixed number of cells (959 somatic cells in the adult hermaphrodite) stereotypically dividing and positioned within the body (Sulston & Horvitz, 1977; Sulston, Schierenberg, White, & Thomson, 1983). The life cycle of *C. elegans* proceeds quickly: development from egg through four larval stages (L1–L4) to fertile adult takes approximately 3 days. Moreover, *C. elegans* reproduces mainly as a self-fertilizing hermaphrodite and under optimal conditions a single adult will produce ~250 progeny over a time course of 3–5 days. For genetic crosses, male animals can be induced by temperature shifts or genetic tricks, allowing classical genetic interaction studies (e.g., complementation or double mutants). *C. elegans* embryos are particularly well suited for analysis of mitotic processes, cell differentiation, and morphogenesis with high temporal and spatial resolution. Surrounded by a resistant eggshell, they can easily be mounted for long time-lapse observation from the zygote to the fast-moving threefold embryo ready to hatch. The first mitotic division is asymmetric, producing two daughter cells of unequal size, composition, and fate. Genetic screens based on this feature have

identified numerous conserved factors involved in polarity establishment through control of mitotic spindle positioning (reviewed in [Gonczy, 2008](#); [McNally, 2013](#)). *C. elegans* can be grown on solid media or in liquid culture, which makes it ideal for high-throughput forward or reverse genetic studies. Genome-wide RNAi screens have for instance uncovered roles of *C. elegans* nucleoporins (nups; in *C. elegans* nomenclature also known as Nuclear Pore Proteins or NPPs) in diverse processes such as transposon silencing ([Vastenhouw et al., 2003](#)), germ granule distribution ([Updike & Strome, 2009](#)) sensitivity to ionizing radiation ([van Haaften et al., 2006](#)). Moreover, the rapid life cycle of *C. elegans* facilitated the striking observation that certain nups are expressed only during embryogenesis and larval development and remain stably integrated in NPCs during the entire lifespan of the animal ([D'Angelo, Raices, Panowski, & Hetzer, 2009](#)).

The above characteristics combined with the fact that most nups ([Table 13.1](#)) and transport factors ([Table 13.2](#)) are conserved in *C. elegans* and that the nuclear envelope disassemble and reassemble at each round of cell division make this organism attractive to study nuclear pore complexes and nucleocytoplasmic transport in a physiological, multicellular but simple *in vivo* context. [Tables 13.1 and 13.2](#) list both general and specific phenotypes ascribed to individual proteins and provide an overview of mutant alleles and available reagents. Scientists who are not familiar with *C. elegans* are encouraged to also consult two recent volumes of *Methods in Cell Biology* dedicated to this model system (vol. 106–107) as well as WormBook available at <http://www.wormbook.org>.

---

## 13.1 FORWARD AND REVERSE GENETICS

*C. elegans* has been extensively used to conduct genetic experiments. Most screens used forward genetics strategies in which animals are mutagenized using chemical or physical DNA-damaging agents. Mutagenized progeny is then screened for the phenotype of interest. Traditionally, positional mapping through genetic crosses, a process that can last several years, was used to identify mutated genes. Forward genetics has recently regained interest with the possibility to rapidly characterize mutations using high-throughput sequencing ([Doitsidou, Poole, Sarin, Bigelow, & Hobert, 2010](#); [Zuryn, Le Gras, Jamet, & Jarriault, 2010](#)). An alternative method to forward genetics is ‘reverse’ screening, in which genes are knocked down individually by RNA interference (RNAi). The creation of genome-wide RNAi libraries made reverse genetic screens easy and cost-efficient ([Kamath & Ahringer, 2003](#); [Rual et al., 2004](#)). Reverse approaches also allow fast and independent confirmation of mutations obtained using forward genetic strategies. While reverse genetic screens are usually faster, forward genetic screens can uncover temperature-sensitive mutations or reduction of function mutants.

Strains carrying deletions for individual genes are available for approximately one third of all protein coding genes. These deletions have mainly been obtained using mutagenesis and PCR-based deletion screening of large strain libraries (<http://www.shigen.nig.ac.jp/c.elegans/>, <http://celeganskoconsortium.omrf.org/>). Such a

**Table 13.1** *C. elegans* nucleoporins

Worm	Human	Frequent phenotypes <sup>a</sup>	Specific phenotypes	Mutant alleles <sup>b</sup>	Reagents <sup>c</sup>	Reference
NPP-1	NUP54	Emb; Lva; Lvl; Nmo; Pgl; Stp	Spindle orientation; RNAi efficiency		FP; Y2H	Kim et al. (2005) and Schetter, Askjaer, Piano, Mattaj, and Kemphues (2006)
NPP-2	NUP85	Clr; Emb; Lva; Nmo; Pgl; Pvl; Stp	NPC assembly; synthetic lethal with NPP-5, -14, -15, -17	<i>tm2199</i>	FP	Galy, Mattaj, and Askjaer (2003) and Rodenas, Gonzalez-Aguilera, Ayuso, and Askjaer (2012)
NPP-3	NUP205	Clr; Emb; Lva; Nmo; Pgl; Ste	NPC exclusion limit; spindle orientation; timing of mitosis	<i>ok1999</i>	Abs; Y2H	Galy et al. (2003), Hachet et al. (2012), and Schetter et al. (2006)
NPP-4	NUPL1	Emb; Stp	Spindle orientation; transposon silencing	<i>ok617</i>	FP; Y2H	Franz et al. (2005), Schetter et al. (2006), Updike, Hachey, Kreher, and Strome (2011), and Vastenhouw et al. (2003)
NPP-5	NUP107	Emb; Pgl	Interaction with spindle assembly checkpoint; kinetochore assembly	<i>ok1966</i> ; <i>tm3039</i>	Abs; FP	Franz et al. (2005) and Rodenas et al. (2012)
NPP-6	NUP160	Emb; Lva; Lvl; Nmo; Pgl	NPC assembly	<i>ok2821</i> ; <i>tm4329</i>	FP	D'Angelo et al. (2009) and Rodenas et al. (2012)
NPP-7	NUP153	Emb; Nmo; Lva; Pgl; Ste		<i>ok601</i>	Abs; FP	D'Angelo et al. (2009), Galy et al. (2003), and Voronina and Seydoux (2010)
NPP-8	NUP155	Emb; Lva; Lvl; Nmo; Pgl; Pvl	NPC assembly	<i>tm2513</i>	Abs; FP	Franz et al. (2005)
NPP-9	NUP358	Emb; Nmo; Pgl; Pvl	RNAi efficiency; spindle assembly;		Abs; FP	Askjaer, Galy, Hannak, and Mattaj (2002), Kim et al. (2005), Sheth, Pitt, Dennis,

NPP-10N <sup>d</sup>	NUP98	Emb; Lva; Lvl; Nmo; Pgl; Ste	nuclear envelope formation NPC assembly; P granule integrity	<i>ok467</i>	Abs; FP	and Priess (2010), and Voronina and Seydoux (2010) Galy et al. (2003), Rodenas et al. (2012), and Voronina and Seydoux (2010)
NPP-10C <sup>d</sup>	NUP96	Emb; Lva; Lvl; Nmo; Ste	NPC assembly		Abs	Galy et al. (2003) and Rodenas et al. (2012)
NPP-11	NUP62	Emb; Lva; Lvl; Nmo	Spindle orientation	<i>ok1599</i>	FP; Y2H	Schetter et al. (2006)
NPP-12	NUP210	Emb; Lva	Nuclear envelope breakdown	<i>ok2424;</i> <i>tm2320</i>	Abs	Audhya, Desai, and Oegema (2007), Cohen, Feinstein, Wilson, and Gruenbaum (2003), and Galy et al. (2008)
NPP-13	NUP93	Emb; Nmo; Pgl	NPC exclusion limit; spindle orientation; timing of mitosis	<i>ok1534</i>	Abs; Y2H	Galy et al. (2003), Hachet et al. (2012), and Schetter et al. (2006)
NPP-14	NUP214	wt	Synthetic lethal with NPP-2	<i>ok1389</i>		Galy et al. (2003)
NPP-15	NUP133	Lvl	Sensitivity to ionizing radiation	<i>ok1954</i>	Abs; FP	D'Angelo et al. (2009), Rodenas et al. (2012), and van Haften et al. (2006)
NPP-16	NUP50	wt	RNAi efficiency; anoxia-induced prophase arrest	<i>ok1839;</i> <i>tm1596</i>		Hajeri, Little, Ladage, and Padilla (2010) and Kim et al. (2005)
NPP-17/ RAE-1	RAE1	Emb; Hya; Pvl; Ste; Stp	Axon termination and synapse formation	<i>ok1720;</i> <i>tm2784;</i> <i>tm2796</i>	Aff; FP	Grill et al. (2012)
NPP-18	SEH1	wt				

Continued

**Table 13.1** *C. elegans* nucleoporins—cont'd

Worm	Human	Frequent phenotypes <sup>a</sup>	Specific phenotypes	Mutant alleles <sup>b</sup>	Reagents <sup>c</sup>	Reference
NPP-19	NUP35	Emb; Nmo; Pgl; Stp	NPC assembly	<i>tm2886</i>	Abs; FP; Y2H	Rodenas et al. (2012) and Rodenas, Klerkx, Ayuso, Audhya, and Askjaer (2009)
NPP-20	SEC13R	Emb; Lva; Lvl; Nmo; Pgl; Stp				
NPP-21	TPR	Clr; Emb; Lva; Ste	Regulation of tumor growth and apoptosis	<i>tm1541</i> ; <i>tm2952</i>		Pinkston-Gosse and Kenyon (2007)
NPP-22 / NDC-1	NDC1 / TMEM48	Clr; Emb; Lva; Lvl; Nmo; Ste	NPC assembly; modification of dynein activity	<i>tm1845</i>	Abs; FP	O'Rourke, Dorfman, Carter, and Bowerman (2007) and Stavru et al. (2006)
NPP-23	NUP43	wt			FP	Rodenas et al. (2012)
MEL-28	ELYS / AHCTF1	Emb; Lva	NPC assembly; spindle assembly	<i>tm2434</i> ; <i>t1578</i> ; <i>t1684</i>	Abs; FP	Fernandez and Piano (2006) and Galy, Askjaer, Franz, Lopez-Iglesias, and Mattaj (2006)

No clear *C. elegans* homologues were found for the mammalian nups AAAS/ALADIN, NUP37, NUP88, NUP188, NUPL2/hCG1, and POM121.

<sup>a</sup>Gross phenotypes, which for most genes were reported in large-scale RNAi studies. See Galy et al. (2003) and WormBase (<http://www.wormbase.org>) for details and references. Clr, clear/transparent body; Emb, embryonic lethal; Hya, hyper active; Lva, larval arrest; Lvl, larval lethal; Nmo, (pro-)nuclear morphology alteration in early embryo; Pgl, P-granule abnormality; Pvl, protruding vulva; Ste, sterile; Stp, sterile progeny; wt, wild type. Abnormal P granule distribution (Pgl) was observed for many npp genes (Updike & Strome, 2009; Voronina & Seydoux, 2010).

<sup>b</sup>Only selected alleles are listed. These and other alleles are available from the Caenorhabditis Genetics Center (CGC; University of Minnesota; <http://www.cbs.umn.edu/CGC/>) and the National Bioresource Project for the Experimental Animal "Nematode *C. elegans*" (Tokyo Women's Medical University School of Medicine; <http://www.shigen.nig.ac.jp/c.elegans/index.jsp>).

<sup>c</sup>Abs, antibodies; Aff, expression of affinity-tagged protein; FP, expression of fluorescently tagged protein; Y2H, plasmids to study yeast two hybrid interactions.

<sup>d</sup>Because NPP-10N and NPP-10C are produced from a single protein precursor, a given RNAi phenotype will generally reflect the combined effect of depleting both proteins. P granule phenotypes are, however, specific to NPP-10N depletion.

**Table 13.2** *C. elegans* transport receptors and Ran GTPase-associated proteins

Worm	Human	Frequent phenotypes <sup>a</sup>	Specific phenotypes	Mutant alleles	Reagents	Reference
IMA-1	KPNA <sup>a</sup>	wt	Silencing of repetitive DNA	<i>gk200</i>	Abs; Aff	Geles and Adam (2001) and Robert, Sijen, van Wolfswinkel, and Plasterk (2005)
IMA-2	KPNA	Emb; Lvl; Nmo	Nuclear envelope formation; spindle assembly	<i>ok256</i>	Abs; Aff	Askjaer et al. (2002) and Geles, Johnson, Jong, and Adam (2002)
IMA-3	KPNA	Emb; Lvl; Nmo; Pgl	NPC assembly; RNAi efficiency; silencing of repetitive DNA	<i>ok715</i>	Abs; Aff	Geles and Adam (2001), Kim et al. (2005), and Robert et al. (2005)
IMB-1	KPNB1/ IMB1	Emb; Nmo	Nuclear envelope formation; spindle assembly		Abs	Askjaer et al. (2002), Fernandez and Piano (2006), and Ikegami and Lieb (2013)
IMB-2	TNPO1/ TRN	Emb; Lva; Lvl; Stp	Redox-dependent nuclear import; RNAi efficiency	<i>tm6328</i>	Abs	Kim et al. (2005) and Putker et al. (2013)
IMB-3	RANBP6	Emb; Lva; Ste		<i>ok1795</i>		
IMB-4/ XPO-1	XPO1/ CRM1	Emb; Lva; Lvl; Pgl; Ste	$\beta$ -Catenin nucl. export; miRNA biogenesis; mRNA export			Bussing, Yang, Lai, and Grosshans (2010), Kuersten, Segal, Verheyden, LaMartina, and Goodwin (2004), Nakamura et al. (2005), and Updike and Strome (2009)
IMB-5/ XPO-2	CSE1L/ CAS	Emb; Lva; Lvl; Nmo; Pgl; Pvl	Chromosome segregation; RNAi efficiency	<i>tm1437</i> ; <i>tm1889</i>		Kim et al. (2005) Updike and Strome (2009), Walther et al. (2003)
IMB-6/ XPO-3	XPOT/ XPO3	wt	Sensitivity to ionizing radiation			van Haaften et al. (2006)

Continued



**Table 13.2** *C. elegans* transport receptors and Ran GTPase-associated proteins—cont'd

Worm	Human	Frequent phenotypes <sup>a</sup>	Specific phenotypes	Mutant alleles	Reagents	Reference
RAN-1	RAN	Emb; Lva; Lvl; Nmo; Pgl; Ste	$\beta$ -Catenin nucl. export; Eph receptor trafficking; nuclear envelope formation; spindle assembly	<i>tm5197</i>	Abs; Aff	Askjaer et al. (2002), Bamba, Bobinnec, Fukuda, and Nishida (2002), Cheng, Govindan, and Greenstein (2008), Nakamura et al. (2005)
RAN-2	RANGAP1	Emb; Nmo; Ste	Nuclear envelope formation; SMN complex component: spindle assembly;	<i>ok1939</i> ; <i>tm3590</i>	Y2H	Askjaer et al. (2002), Bamba et al. (2002), and Burt, Towers, and Sattelle (2006)
RAN-3	RCC1	Emb; Lvl; Nmo; Pvl; Ste	$\beta$ -Catenin nucl. export; nuclear envelope formation; RNAi efficiency	<i>ok3709</i>	FP	Askjaer et al. (2002), Bamba et al. (2002), Kim and Yu (2011), and Nakamura et al. (2005)
RAN-4	NUTF2/ NTF2	Emb; Lva; Nmo; Pgl; Ste		<i>tm1439</i>		Updike and Strome (2009)
RAN-5	RANBP3	Nmo	$\beta$ -Catenin nucl. export			Nakamura et al. (2005)

Annotated *C. elegans* importins, exportins, and Ran GTPase-related proteins. Other transport factors, such as *RXF-1*, *-2*, *ALY-1*, *-2*, *-3*, etc., are omitted due to space constraints. See [Table 13.1](#) for column legends.

<sup>a</sup>The homology between *C. elegans* IMA proteins and human importin alpha (KPNA) proteins is insufficient to make pair-wise assignments (Geles et al., 2002).

strategy has the intrinsic drawback that the rest of the genome is mutagenized too. Mutants therefore have to be outcrossed extensively to wild-type strains to clean the genetic background. This remains very inefficient for linked mutations and a few background 'equilibrating' mutations can persist over a number of backcrosses. To overcome this and create targeted short deletions, the newly developed CRISPR-Cas9 system has been adapted for use in *C. elegans* (Chiu, Schwartz, Antoshechkin, & Sternberg, 2013; Friedland et al., 2013; Lo et al., 2013; Waaijers et al., 2013). Cas9 is an RNA-guided nuclease, which induces a sequence-specific double strand break that when repaired by nonhomologous end joining creates small insertions and deletions. The efficiency appears high enough that the technique is likely to become routine in the next years. Moreover, when oligonucleotides spanning over the break site are coinjected with CRISPR-Cas9, the repair machinery is able to use these as a template for repair, enabling the creation of targeted point mutations in the genome.

### 13.1.1 RNAi

The discovery of RNAi as means to efficiently knockdown expression of individual genes (Fire et al., 1998) increased dramatically the popularity of *C. elegans*. Despite that RNAi-based tools are now available in many systems, *C. elegans* is still an attractive organism to induce and study loss-of-function phenotypes (Simpson, Davis, & Boag, 2012). RNAi efficiency is remarkably high and persists through generations due to an endogenous amplification step mediated by RNA-dependent RNA polymerases found in nematodes, fungi, and plants. Moreover, RNAi in *C. elegans* spreads throughout the body (although with a lower effect in the nervous system) causing a systemic knockdown. Finally, *C. elegans* can easily be cultivated in liquid in 96-well plates, thus facilitating genome-wide scale studies.

Three methods have been developed to introduce the triggering double-stranded RNA (dsRNA) in *C. elegans*: (1) injection of dsRNA into the nematodes, (2) soaking of the nematodes in a solution containing dsRNA, and (3) feeding bacteria expressing the dsRNA to the nematodes. The injection and soaking methods both require *in vitro* dsRNA synthesis and purification and the former also necessitates dedicated microinjection equipment and training. The feeding method relies on simple cloning and microbiology techniques and is easily scaled up in terms of quantity of nematodes and/or number of genes to be analyzed. Moreover, bacteria clones can be amplified and distributed inexpensively. We therefore focus here on the feeding method, but the reader should keep in mind that the efficiency in some cases have been found to be slightly inferior to injection. Hence, if by feeding an expected phenotype is not observed or if quantification shows an incomplete depletion, injection, or soaking should be considered. The protocol below is designed to analyze a few genes. An in-depth discussion of methods and protocols for large-scale RNAi screening is available (Cipriani & Piano, 2011).

Bacteria expressing dsRNA corresponding to the gene(s) to be analyzed can be generated by standard molecular biology techniques, obtained from a *C. elegans* laboratory that possesses the relevant clone(s) or, for most annotated genes, purchased

(e.g., Source BioScience [<http://www.lifesciences.sourcebioscience.com>] or Thermo Scientific [<http://www.thermoscientificbio.com>]).

### 13.1.2 Construction of RNAi clone

1. Design PCR primers to amplify a 300- to 1000-bp fragment of your gene. If you use genomic DNA as template place the primers to get maximum exon content. Alternatively, use cDNA as template. BLAST your fragment against the *C. elegans* genome (e.g., at <http://www.wormbase.org>) to ensure that the fragment does not target other genes (avoid matching sequences >20 nt). Add restriction sites to the primers to facilitate insertion of the fragment between the two convergent T7 promoters of the vector pPD129.36 L4440 (available from <http://www.addgene.org> or any *C. elegans* lab).
2. Restriction digest, purify, and ligate PCR fragment(s) and vector.
3. Transform the ligation reaction into standard bacteria and plate on LB-Amp plates.
4. Miniprep DNA from several colonies and check for correct insert.
5. Transform HT115(DE3) bacteria with miniprep DNA. Include also a reaction with pPD129.36 to use as negative RNAi control. HT115(DE3) is RNase III-Tet<sup>+</sup> and can be obtained from the Caenorhabditis Genetics Center (<http://www.cgc.cbs.umn.edu>). Plate on LB-Amp-Tet (optional: using carbenicillin instead of ampicillin may improve RNAi efficiency due to higher stability of this antibiotics).

### 13.1.3 Preparation of RNAi plates

1. Inoculate 3 ml LB-Amp with a single colony from a fresh LB-Amp-Tet plate and incubate at 37 °C, 200 rpm until OD<sub>600</sub> = 0.6–0.8 (~8 h). Alternatively, grow bacteria overnight.
2. Add 1 mM IPTG to the bacteria culture just before seeding the plates.
3. Seed NGM plates containing 1 mM IPTG and 100 µg/ml ampicillin or 20 µg/ml carbenicillin with 100 µl of bacteria culture.
4. Incubate at room temperature overnight and use immediately or store at 16 °C for a few days.

### 13.1.4 *C. elegans* RNAi feeding

1. In the days prior to the experiment check that worms are growing well without suffering starvation or contamination.
2. Transfer worms to an empty NGM plate and leave for 30–60 min remove bacteria sticking to the cuticle. Select L4 larvae for analysis of RNAi-depleted embryos.
3. Transfer 10–15 L4s to RNAi plates (optional: after the worms have moved away from the spot on the RNAi plate where they were placed, put 5 µl of 50% household bleach/1 N NaOH solution to kill any bacteria transferred with the worms).

4. Incubate plates for 16–48 h at 16–25 °C. For several genes RNAi efficiency has been observed to be temperature-dependent so it is advisable to test several conditions. Likewise, kinetics of protein synthesis and turnover will influence the rate of RNAi-mediated depletion.
5. Dissect worms to obtain embryos for live imaging as described below. To study postembryonic phenotypes adult worms should be transferred to fresh RNAi plates every 12–24 h to generate semisynchronous populations of offspring.

### 13.1.5 Materials

#### *C. elegans* genomic DNA as PCR template

For 1–few reactions, sufficient DNA can be obtained by disrupting 5–10 worms in a PCR tube containing 2.5 µl lysis buffer. Overlay with a drop of mineral oil to prevent evaporation. Incubate at –80 °C for 15 min; 60 °C for 1 h; 95 °C for 15 min. Add 22.5 µl PCR mixture to PCR tube with lysed worms (for amplification of a single target sequence) or dilute and split lysed worms in 2–5 PCR tubes (for several target sequences).

#### Worm lysis buffer

Tris/HCl 10 mM pH 8.3

KCl 50 mM

MgCl<sub>2</sub> 2.5 mM

NP-40 0.45%

Tween-20 0.45%

Gelatin 0.01%

Add 1 µl proteinase K (10 mg/ml; Sigma P6556) to 99 µl of worm lysis buffer immediately before use

#### NGM plates

NaCl 50 mM

Agar 1.7%

Peptone 0.25%

Autoclave and add sterile

Cholesterol (5 mg/ml in EtOH) 1 ml/L

CaCl<sub>2</sub> 1 mM

MgSO<sub>4</sub> 1 mM

Potassium phosphate pH 6.0 25 mM

For RNAi add 1 mM IPTG and 100 µg/ml ampicillin or 20 µg/ml carbenicillin

---

## 13.2 TRANSGENESIS

Transgenesis in *C. elegans* has greatly improved in the last few years, offering a variety of methods with different advantages and limitations (Table 13.3). The simplest and most frequently used transgenes are extrachromosomal arrays.

**Table 13.3** Comparison of transgene types

<b>Transgene type</b>	<b>Extrachromosomal arrays</b>	<b>Integrated extrachromosomal array</b>	<b>Bombarded transgenes</b>	<b>Homologous recombination<sup>a</sup></b>
Size	Very large (>100 copies)	Very large (>100 copies)	From 1 to 100 copies	Single insertion
Insertion site	Extrachromosomal	Random insertion	Random insertion	Targeted insertion
Chromatin state	Heterochromatic	Heterochromatic	Variable	Variable
Mitotic and meiotic stability	Variable	100% stable	100% stable	100% stable
Expression level	Usually high to very high expression levels	Usually high to very high expression levels	Low/middle expression levels	Low (endogenous) expression levels
Germline/early embryo expression	Usually silenced	Usually silenced	Variable (promoter dependent)	Usually expressed (insertion site dependent)
Nature of exogenous DNA	Mixture of plasmids	Uses an extrachromosomal array	Mixture of plasmids	Mixture of plasmids/homologous recombination template
Mode of transgenesis	Injection	Irradiation (UV/X-ray)	Bombardment	Injection
Genome mutagenic load	None	High (extensive backcrossing recommended)	Low (backcrossing recommended)	Low (backcrossing recommended)
Price	Inexpensive	Inexpensive	Expensive	Inexpensive
Difficulty/workload	Easy and fast	Labor intensive (selection and backcrossing)	Labor intensive (worm amplification)	Labor intensive (large number of injections)

<sup>a</sup>Homologous recombination through repair of a double-stranded DNA break can be initiated either by *Mos1* transposase or RNA-guided Cas9 nuclease activity. Insertion site is based on the presence of *Mos1* transposons in the genome or design of small guide RNA molecules. See text for details.

Extrachromosomal arrays are created by injection of DNA inside the worm gonad. Injected DNA is concatenated into an array which stability varies both mitotically and meiotically, depending on its sequence composition and complexity. Transgenic worms are identified either by a fluorescent or phenotypic marker or by the rescue of a mutation. Due to their high copy number, expression from arrays is usually very high (overexpressed) and in the case of fluorescent proteins readily observed with a dissecting scope. However, arrays are usually poorly expressed in the germline and early embryos, most likely because of their highly repetitive nature and their heterochromatic structure. A number of strategies can be employed to increase complexity, improve stability, and germline expression of the arrays, for instance by coinjecting heterologous DNA. Arrays can also be integrated into the genome by irradiation and screening for stable transmission. The method for germline injection is extensively described (Berkowitz, Knight, Caldwell, & Caldwell, 2008).

An alternative to injected arrays is microparticle bombardment (Hochbaum, Ferguson, & Fisher, 2010; Praitis, 2006). Gold beads coated with DNA are shot at worms and occasionally the bombarded DNA gets randomly integrated into the genome. Germline integration is recognized by 100% transmission to the progeny and/or rescue of a phenotypically screenable mutation. Transgene arrays obtained by bombardment are smaller in size, ranging from 1 to 100 copies and less subject to germline silencing. The drawbacks of the bombardment method is the cost of the device and consumables as well as the difficulty to check for homozygosity when crossing strains as the insertion site is most often unknown.

To avoid insertion-site artifacts and better control copy number, site-specific integration of transgenes using homologous recombination was recently developed. These methods are based on induction of a site-specific DNA double strand break through the action of either Mos1 transposase or Cas9 nuclease. In Mos1-mediated single-copy insertion (MosSCI) and Mos1 excision induced transgene-instructed gene conversion (MosTIC), the transposase is expressed in a strain harboring a characterized insertion of the *Drosophila* transposon Mos1 (Frokjaer-Jensen, Davis, Ailion, & Jorgensen, 2012; Frokjaer-Jensen et al., 2008; Robert & Bessereau, 2011). More than 13,000 individual Mos1 insertion sites have been isolated, which in principle can all be used for genetic engineering (Vallin et al., 2012). The CRISPR-Cas9 method allows even more flexibility because the system can be designed to cleave the genome specifically at any site that contains a G/A(N)<sub>19</sub>NGG sequence motif (Chen, Fenk, & de Bono, 2013; Dickinson, Ward, Reiner, & Goldstein, 2013; Katic & Grosshans, 2013; Tzur et al., 2013). In both methods, a transgene surrounded by sequences homologous to the flanking sequences of the break is injected into the germline and serves as template for recombination repair. Depending on the design of the repair template, the methods can be used to introduce transgenes into intergenic regions of the genome or to tag endogenous loci. To discriminate between homologous recombination and the creation of an array, additional markers are injected, which can later be counter-selected. Detailed protocols for both methods, including tools to identify suitable CRISPR-Cas9 target sequences, are available online

(e.g., <https://sites.google.com/site/jorgensenmossaci/>; <http://wormcas9hr.weebly.com>; <http://crispr.mit.edu>). Although Mos1- and CRISPR-Cas9-mediated homologous recombination offer the advantage of mimicking endogenous expression levels, detection of weakly expressed fluorescent constructs may be challenging.

When transgenes should be expressed only in some cells, a number of characterized promoters are available for expression in differentiated somatic tissues. Expression in these cells is usually not an issue, although using heterologous, cell-type specific promoters might lead to overexpression. The germline and the early embryo remain the most difficult tissues to express transgenes, due to mechanisms defending the genome against exogenous DNA. As stated above, arrays are usually not expressed at that stage, while bombarded and single-copy transgenes have variable expression success. Promoters that have been shown proficient for expression in the germline include *pie-1* and *mex-5* (Merritt, Gallo, Rasoloson, & Seydoux, 2010; Zeiser, Frokjaer-Jensen, Jorgensen, & Ahringer, 2011). Other promoters (e.g., housekeeping genes, such as *tbb-1*, *baf-1*, *his-72*) can also efficiently drive expression in the germline, but get silenced more often.

---

### 13.3 LIVE IMAGING OF EMBRYOS

Live imaging of early *C. elegans* embryos is a powerful way to examine the consequences of an RNAi depletion or mutation of a given nuclear pore complex (NPC) component by DIC microscopy (Galy et al., 2003; Sonnichsen et al., 2005) or fluorescence microscopy (Galy et al., 2003). Many different read-outs allow detecting defects in protein nuclear import, nuclear envelope (NE), and NPC integrity (Askjaer et al., 2002; D'Angelo et al., 2009; Galy et al., 2003), and NPC distribution (Lee, Gruenbaum, Spann, Liu, & Wilson, 2000) (Tables 13.1, 13.2, 13.4, and 13.5). Furthermore, imaging of embryos expressing NPC or NE components fused to green fluorescent protein (GFP) provide information about the timing of their insertion during postmitotic NE formation (Franz et al., 2005) as well as their turnover at the NE (Galy et al., 2006). Importantly, validation of these fluorescent reporters as reliable reporters for their endogenous counterparts is facilitated by the availability of knock-out alleles in public repositories (see Section 13.1.1 and Tables 13.1 and 13.2).

Fertilization naturally occurs inside the worm body every ~20 min in each of the two gonad arms. This is followed within half an hour by the completion of meiosis, pronuclear formation, meeting, and centration and finally the first mitotic cell division (Fig. 13.1). Completion of meiosis is coordinated with the production of the chitin-containing eggshell that protects and isolates the embryo from the external environment and physical constrains (Olson, Greenan, Desai, Muller-Reichert, & Oegema, 2012). This timing is important to consider since drugs and lipophilic fluorescent dyes are able to enter the embryo only prior to egg-shell synthesis simply by soaking early meiotic embryos. Alternatively, drugs and dyes can be injected into the gonads of the hermaphrodite a few hours before collecting the embryos for imaging (Galy et al., 2003). For exposure of embryos at a given time-point, the egg-shell may

**Table 13.4** Useful fluorescent markers

Strain	Reporter	Tissue	Comments	Reference
BN46	GFP:: NPP-19	Embryos and germ line	GFP:: <npp-19 (nup35)<br=""></npp-19> accumulates in germ line and embryonic NEs; endogenous <i>npp-19</i> is mutated but rescued by GFP:: <npp-19 expression<="" td=""> <td>Rodenas et al. (2009)</td> </npp-19>	Rodenas et al. (2009)
BN69	GFP:: NPP-5	Embryos and germ line	GFP:: <npp-5 (nup107)<br=""></npp-5> accumulates in germ line and embryonic NEs; endogenous <i>npp-5</i> is mutated but rescued by GFP:: <npp-5 expression;<br=""></npp-5> co-expression of mCherry::HIS- 58	Rodenas et al. (2012)
GZ264	GFP:: PCN-1	Embryos and oocytes	GFP:: <pcn-1 (pcna)<br=""></pcn-1> accumulates in all embryonic nuclei	Brauchle, Baumer, and Gonczy (2003)
JH1327	PIE-1:: GFP	Embryos and oocytes	PIE-1:: <gfp accumulates="" in="" the<br=""></gfp> germ line blastomer where it is imported into the nucleus	Reese, Dunn, Waddle, and Seydoux (2000)
MR164	NLS:: GFP	Intestine	Bright signal; strains carries also <i>lin-35</i> mutation	Kostic and Roy (2002)
OD83	GFP:: LEM-2	Embryos and germ line	GFP:: <lem-2 accumulates="" in<br=""></lem-2> germ line and embryonic NEs; co-expression of mCherry::HIS- 58	Audhya et al. (2007)
OD139	YFP:: LMN-1	Embryos and germ line	YFP:: <lmn-1 (lamin)<br=""></lmn-1> accumulates in germ line and embryonic NEs; co-expression of mCherry::HIS-58	Audhya et al. (2007)
PS3808	NLS:: GFP:: LacZ	Uterus, vulva and neurons	Bright signal; expression restricted to specific cell types within these tissues	Gupta and Sternberg (2002)
WH204	GFP:: TBB-2	Embryos and germ line	Bright expression of GFP:: <tbb-2 </tbb-2  ( $\beta$ -tubulin); useful to analyze nuclear exclusion of soluble tubulin	Strome et al. (2001)

*Nonexhaustive list of strains expressing NE or nuclear import markers. All strains are available from the Caenorhabditis Genetics Center (CGC; University of Minnesota; <http://www.cbs.umn.edu/CGC/>).*

physically be disrupted by applying a gentle pressure on the embryo (Gonczy et al., 2001) or by *perm-1* RNAi, which when combined with immobilized embryos allows precisely timed drug inhibitions (Carvalho et al., 2011). In the latter study, a custom-build microdevice consisting of an array of wells (300  $\mu\text{m}$   $\times$  300  $\mu\text{m}$  and 150  $\mu\text{m}$  deep) was used to exchange a neutral medium for a drug-containing medium (or vice

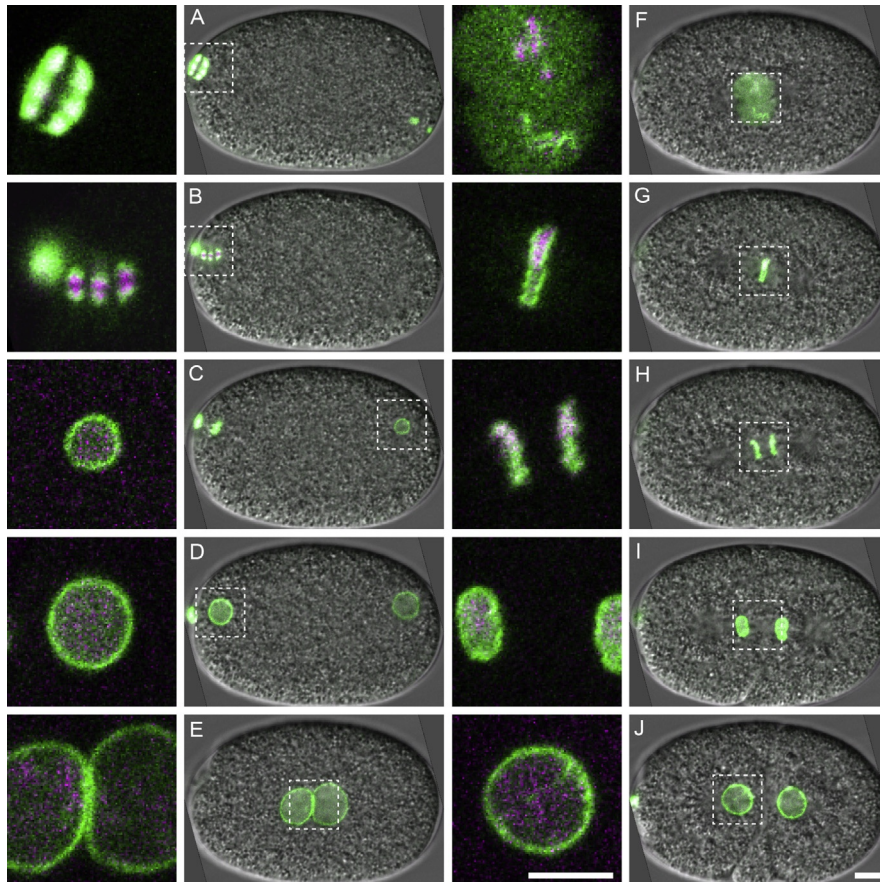


Antigen	Code <sup>a</sup>	Type <sup>b</sup>	IF <sup>c</sup>	WB <sup>c</sup>	IP <sup>c</sup>	Source	Reference
Actin	C4	Mm	+			MP Biomedicals	
EMR-1	3272	Mp	+	+			Gruenbaum, Lee, Liu, Cohen, and Wilson (2002)
	3598	Rp	+				Gruenbaum et al. (2002)
FG nups	MAb414	Mm	+	+		Abcam, Covance	Galy et al. (2003)
GFP	D153-3	Rm	+	+		MBL	Rohner et al. (2013)
IMB-1	SDQ4154; 4155	Lp*			+	Novus Biologicals	Ikegami and Lieb (2013)
LEM-2	Q3891; Q4051	Lp*	+	+	+	Novus Biologicals	Ikegami, Egelhofer, Strome, and Lieb (2010)
	3597	Rp	+				Gruenbaum et al. (2002)
LMN-1	SDQ2349	Lp*		+		Novus Biologicals	Ikegami and Lieb (2013)
	3932	Lp*	+	+	+		Gruenbaum et al. (2002)
	LMN1	Mm	+	+		The Developmental Studies Hybridoma Bank	Hadwiger, Dour, Arur, Fox, and Nonet (2010)
MEL-28	BUD3	Lp*	+	+			Galy et al. (2006)
	MEL28	Lp*	+				Fernandez and Piano (2006)
NPP-3	SY1539; 1540	Lp*	+		+		Hachet et al. (2012) and Ikegami and Lieb (2013)
NPP-5	SG4839	Lp*	+	+			Rodenas et al. (2012)
NPP-9	P5A6	Mm	+	+			Sheth et al. (2010)
	SDQ3854	Lp*	+			Novus Biologicals	

NPP-10N	Ab#1; Ab#2	Cp	+	+		Voronina and Seydoux (2010)	
	GBJQ	Lp	+	+		Galy et al. (2003)	
NPP-10C	GBLC	Lp	+	+		Galy et al. (2003)	
NPP-12	NPP12	Lp	+	+		Galy et al. (2008)	
NPP-13	SDQ3897; 4094	Lp*			+	Novus Biologicals	Ikegami and Lieb (2013)
	JL00007	Lp*			+		Ikegami and Lieb (2013)
	NPP13	Lp*	+				Hachet et al. (2012)
NPP-16	SDQ3896; 4093	Lp*	+	+		Novus Biologicals	
NPP-19	OWYL	Lp*	+	+			Rodenas et al. (2009)
SUN-1	41970002	Lp*	+	+		Novus Biologicals	
$\alpha$ -Tubulin	DM1a	Mm	+	+		Sigma	Askjaer et al. (2002)
	12G10	Mm	+			The Developmental Studies Hybridoma Bank	Fernandez and Piano (2006)
Unknown NE antigen	AB18251	Lp*	+	+		Abcam	
	KT23	Mm	+			The Developmental Studies Hybridoma Bank	Takeda, Watanabe, Qadota, Hanazawa, and Sugimoto (2008)
<p><i>Nonexhaustive list of antibodies that efficiently recognize C. elegans antigens. Please refer to Tables 13.1 and 13.2 for a complete listing of NE-related proteins for which antibodies are available.</i></p> <p><sup>a</sup>Code of serum, antibody batch, or monoclonal description.</p> <p><sup>b</sup>Cp, guinea pig polyclonal; Lp, rabbit polyclonal; Lp*, affinity purified rabbit polyclonal; Mm, mouse monoclonal; Mp, mouse polyclonal; Rm, rat monoclonal; Rp, rat polyclonal.</p> <p><sup>c</sup>IF, immunofluorescence; WB, western blot; IP, immunoprecipitation.</p>							

versa) in  $\sim 1$  min with constant observation of the samples (see [Carvalho et al., 2011](#) for details).

Drugs that have been successfully utilized in *C. elegans* through any of these delivery methods include nocodazole to destabilize microtubules (10–100  $\mu\text{g/ml}$ , Sigma M1404; [Gonczy et al., 2001](#)), latrunculin A to inhibit actin (10  $\mu\text{M}$ , Sigma

**FIGURE 13.1**

Time-lapse observation of nucleoporin dynamics. Selected still images from confocal time-lapse recording of *C. elegans npp-5* (NUP107) mutant embryo expressing a rescuing GFP::NPP-5 fusion protein (green) and mCherry::HIS-58 (hisH2B; magenta) (Rodenas et al., 2012). Boxed regions in the merged panels are shown at higher magnification to the left. Embryo is mounted with anterior to the left. (A) GFP::NPP-5 localize to separating chromosomes in meiosis I (anterior) and to sperm-derived chromatin (posterior,  $\sim 5 \mu\text{m}$  from cortex); (B) GFP::NPP-5 accumulates on kinetochores during meiosis II; (C) NE assembly around sperm-derived chromatin; (D) NE assembly around oocyte-derived chromatin; (E) juxtapositioning of fully grown pronuclei; (F) NE breakdown and accumulation of GFP::NPP-5 at kinetochores of condensing chromosomes in prometaphase; (G) GFP::NPP-5 localizes to kinetochores of holocentric chromosomes, which are arranged as two straight lines facing the mitotic spindle poles in metaphase; (H) signal of GFP::NPP-5 spreads to cover chromosomes in anaphase; (I) enrichment of GFP::NPP-5 at the nuclear periphery during NE reassembly in telophase; and (J) nuclear growth in interphase. Bars,  $5 \mu\text{m}$ .

L5163; [Carvalho et al., 2011](#)), the proteasome inhibitor c-lactocystin- $\beta$ -lactone (20  $\mu$ M, Calbiochem 426102; [Carvalho et al., 2011](#)), and the XPO-1 (CRM1) inhibitor leptomycin B (1 ng/ml, Sigma L2913; [Pushpa, Kumar, & Subramaniam, 2013](#)).

### 13.3.1 Sample preparation

Embryos are extracted by dissection of gravid hermaphrodites in a drop of appropriate physiological buffer. Embryos that have completed meiosis (>30 min post fertilization) at the time of dissection will survive in M9 buffer, while earlier embryos devoid of a mature egg-shell are sensitive to physical and osmotic pressure and require meiosis buffer or egg salts to develop.

1. Using a worm pick, transfer one to five young adult gravid hermaphrodites to a 25- $\mu$ l drop of buffer to remove bacteria.
2. Transfer the worms to a 5- $\mu$ l drop of buffer on a 22-mm square glass coverslip.
3. Cut the worms in the middle using thin forceps (Dumont N<sup>o</sup>5) and a syringe needle (26 GA) to release the embryos from the uterus.
4. Collect gently the embryos by approaching and contacting the drop of buffer with a freshly made wet agarose pad (2% agarose in water or meiosis buffer lacking FBS) on a slide.
5. Seal the coverslip using melted VALAP.
6. For optimum temperature control during the live imaging, glue the slide onto a fast response temperature controller using a thin layer of vacuum grease. Recordings are typically performed at 20 °C to minimize the risk of local overheating but the temperature controller may be set up to temperatures ranging from 16 to 25 °C and allows rapid temperature shifts to analyze temperature-sensitive mutants ([Gorjanacz et al., 2007](#)). However, when DIC imaging is required we recommend to not use the temperature controller.
7. Place a drop of immersion oil on the coverslip and put the slide onto the microscope. Using a low magnification objective, quickly select a suitable one-cell stage embryo and switch to a 63 $\times$  or 100 $\times$  oil objective for recording with the best possible image resolution using fluorescent microscopy.

### 13.3.2 How to limit phototoxicity

As a good practice, effects of illumination on embryogenesis should be assayed. Under appropriate live imaging conditions, the monitored embryos develop normally (no defects in asymmetric cell divisions, timing of cell division nor chromatin segregation) and hatch under the coverslip after 12–14 h. Minimizing the light dose applied to the specimen is critical to reduce photobleaching and associated phototoxicity. Laser power should be kept at a minimum value and the number of slides in Z stacks as well as frequency of the stacks should be limited to what is strictly required. For a given dose of light it causes less damage when delivered slowly (increased exposure time with reduced laser power or light intensity) ([Tinevez et al., 2012](#)). Typically, a 488-nm laser power <0.2 mW/cm<sup>2</sup> before the

objective allows to record early embryogenesis in 3D stacks of 10–15 images every minute. Epifluorescent microscopy, conventional, or two-photon laser scanning microscopy as well as spinning disk confocal microscopy may be used for live imaging with time interval typically ranging from 5 s to 1 min. A spinning disk confocal equipped with a back illuminated EM-CCD camera offers a good compromise for high temporal resolution and 3D imaging in one or two fluorescent channels.

While imaging nuclei in a single confocal plane is sufficient to analyze the distribution of NE and NPC components or to estimate the nuclear size in wild-type embryos up to the four-cell stage, 3D imaging is required when embryos display an altered nuclear morphology or positioning or for later multicellular stages. Considering that NE or NPC defects might trigger a range of secondary or cumulative defects as the embryo develops, it is recommended to analyze the primary defects as early as in the one-cell stage.

### 13.3.3 Materials

#### M9 buffer

$\text{KH}_2\text{PO}_4$  22 mM

$\text{Na}_2\text{HPO}_4$  50 mM

NaCl 85 mM

$\text{MgSO}_4$  1 mM

#### Meiosis buffer

Inulin 0.5 mg/ml

HEPES 25 mM pH 7.4

Leibovitz L-15 Medium 60%

Fetal bovine serum [FBS] 20%

#### Egg salts

HEPES 5 mM pH 7.4

NaCl 118 mM

KCl 40 mM

$\text{MgCl}_2$  3.4 mM

$\text{CaCl}_2$  3.4 mM

#### VALAP

1:1:1 mixture of Vaseline or petroleum jelly, lanolin, and paraffin; melts at 60 °C.

Fast Response Mini Stage Temperature Controller

Manufactured by EMBL (<http://www.embl-em.de>) Ref.-No. 396.

---

## 13.4 *IN VIVO* METHODS TO EVALUATE STRUCTURAL AND FUNCTIONAL INTEGRITY OF THE NE

NE structural and functional integrity can be monitored in living embryos by testing its ability to import nuclear proteins and exclude large soluble molecules from the nuclear space during interphase. GFP-tagged  $\alpha$ - or  $\beta$ -tubulin expressed in the

germline from the *pie-1* promoter is not present in the nucleus prior to NE breakdown except when NPC (Galy et al., 2003) or NE integrity (Askjaer et al., 2002; Gorjanacz et al., 2007) is impaired (Fig. 13.2B). Alternatively, fluorescently labeled dextrans can be used to measure the exclusion limit imposed by the NE and NPCs. Dextran of 10 kDa accumulates in the nuclear space by passive diffusion through the NPCs while 70 kDa or larger dextrans are excluded from nuclei during interphase (Fig. 13.2A). A 1:1 mixture of two differentially labeled dextrans (see protocol below) is injected into one of the syncytial gonads of the animals, followed by incubation at 20 °C for 5 h before dissection. The distribution of the fluorescent

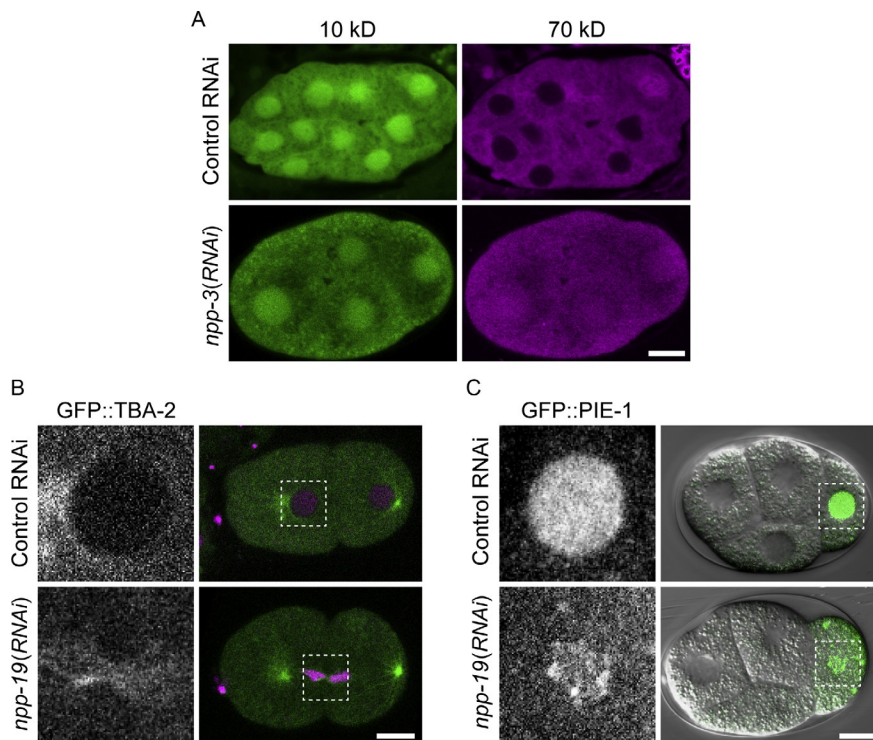


**FIGURE 13.2**

Methods to evaluate NE integrity and function. (A) Gonads of control and *npp-3* (NUP205) depleted animals were injected with a mix of fluorescent dextrans of 10 kDa (left) and 70 kDa (right). The 10-kDa dextran diffused freely into all nuclei, whereas the 70-kDa dextran was only excluded from nuclei of control embryos and not from nuclei of *npp-3(RNAi)* embryos. (B and C) Control and *npp-19*/NUP35 depleted embryos expressing mCherry::HIS-58 (hisH2B; magenta) and GFP::TBA-2 ( $\alpha$ -tubulin; green) (B) or GFP::PIE-1 (green) (C). Boxed regions in the merged panels are shown at higher magnification to the left. Nuclei of *npp-19(RNAi)* embryos do not exclude soluble tubulin nor efficiently import PIE-1. Bars, 10  $\mu$ m.

(A) Adapted from Galy et al. (2003) and (B and C) Rodenas et al. (2009), with permission from Elsevier.

dextran in newly formed embryos is monitored by live confocal microscopy. Comparing the nucleocytoplasmic distribution of 70 kDa to a 155-kDa (Rodenas et al., 2012) or larger dextran (up to 500 kDa; D'Angelo et al., 2009) allows to discriminate between altered NPC permeability barrier and NE structural defects. The 70-kDa dextran may enter the nuclear space upon modification of NPC structure (D'Angelo et al., 2009; Galy et al., 2003) while the larger dextrans enter the nuclear space only upon overall defects in NE integrity (Gorjanacz et al., 2007).

### 13.4.1 Preparation of fluorescently labeled dextran for germline injection

1. Dissolve dextrans (e.g., Rhodamine-labeled 10-kDa dextran [Sigma R8881], FITC-labeled 70-kDa dextran [Sigma FD70S], and TRITC-labeled 155-kDa dextran [Sigma T1287]) in phosphate-buffered saline (PBS) or injection buffer (20 mM KPO<sub>4</sub>, pH 7.5; 3 mM K Citrate, pH 7.5; 2% polyethylene glycol 6000) to a concentration of 0.2 mg/ml.
2. To remove free dye, spin dextrans in Nanosep 10 K columns (or 3 K column for 10-kDa dextran) at 5000 × *g* until sample volume is reduced to ~10%.
3. Dilute sample 10-fold with PBS or injection buffer and repeat centrifugation until a final concentration of 2 mg/ml in phosphate-buffered saline.
4. Purified dextrans can be injected immediately or stored at –20 °C.

Classical nuclear import reporters, such as SV40 NLS fused to GFP, are available for a variety of somatic tissues (see e.g., Bamba et al., 2002; Rodenas et al., 2012) but are not expressed in early embryos. Instead, bulk nuclear protein import can be estimated by measuring the increase of nuclear volume or the average maximum size of the nucleus in P1 blastomeres of two-cell stage embryos (Galy et al., 2003). Alternatively the intensity of nuclear PIE-1::GFP signal in P2 blastomeres of four-cell stage embryos as well as the increase of nuclear PCNA::GFP intensity (Rodenas et al., 2012) or the import of YFP::lamin (Galy et al., 2003) may be used to evaluate the efficiency of nuclear protein import (Fig. 13.2C). While single RNA molecule detection is feasible on fixed embryos (Raj, van den Bogaard, Rifkin, van Oudenaarden, & Tyagi, 2008), a major challenge to live cell imaging is to label RNAs in embryos *in vivo* using either injection in the worm gonads of fluorescently labeled RNA probes or molecular beacons. A possible alternative would be to use the MS2 system requiring the expression of the fusion of the MS2 coat protein to a fluorescent protein and a reporter RNA containing several copies of the RNA stem-loop recognized by the MS2 coat protein (Querido & Chartrand, 2008).

---

## 13.5 IMMUNOFLUORESCENCE AND ELECTRON MICROSCOPY

NE structure and composition can be studied at high resolution in fixed samples by immunofluorescence or transmission electron microscopy. Protocols have also been established for Correlative Light and Electron Microscopy of one-cell stage embryos

and may be directly applicable to NE and NPC analysis (Woog, White, Buchner, Srayko, & Muller-Reichert, 2012). Several commercial antibodies raised against proteins from other species work well in *C. elegans* (e.g., antitubulin and anti-RAN antibodies, MAb414; Table 13.5). Antibodies against specific *C. elegans* NE-related proteins are listed in Tables 13.1, 13.2, and 13.5.

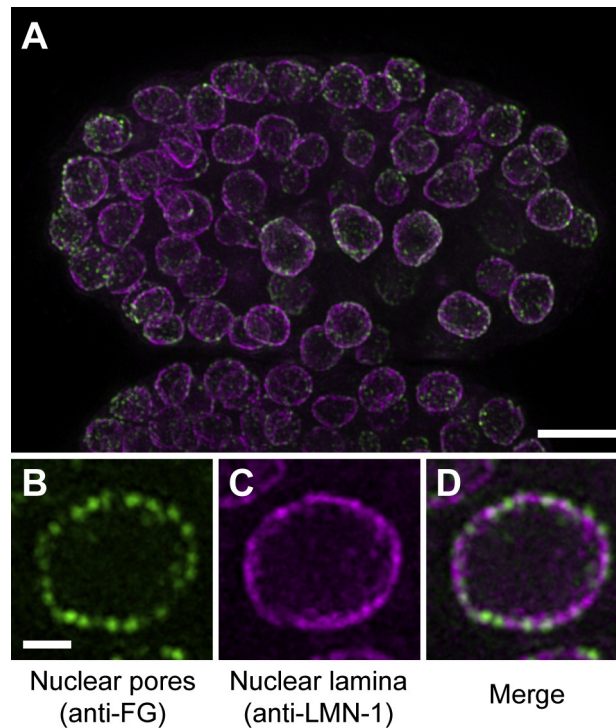
### 13.5.1 Immunofluorescence

Visualization of protein localization by immunofluorescence in *C. elegans* follows similar protocols as for other sample types, except for permeabilization. The protocol below involves a freeze-crack step to rupture the eggshell of embryos whereas procedures to penetrate the cuticle of larvae and adults can be consulted elsewhere (Shakes, Miller, & Nonet, 2012). The protocol is suitable for observation by classical epifluorescence microscopy as well as by advanced super-resolution microscopy, the latter allowing visualization of individual NPCs and precise evaluation of NPC density in the NE. Although a number of super-resolution techniques are available with claimed resolution ranging from 100 to 40 nm, the 100-nm resolution obtained using super-resolution structured illumination microscopy (SR-SIM) is sufficient to detect single pores and to discriminate between two closely located perinuclear structures, such as the nuclear lamina and NPCs (Fig. 13.3).

#### FIXATION

1. Prepare fresh poly-lysine slides by coating microscope slides with 0.01% poly-lysine (Sigma P9820 diluted 1:10). Spread poly-lysine with a rubber policeman/scrapper and put on a  $\sim 200$  °C heating plate. Remove once water has evaporated and use immediately.
2. Starting from 2 to 4 10 cm plates full of gravid adults, wash plates with 10 ml of M9 buffer, passing buffer from one plate to the next. Put M9 with worms in a 15-ml conical tube.
3. Pellet worms by centrifugation (1000 g, 2 min), aspirate supernatant.
4. Prepare bleach solution by adding 0.5 ml bleach (Sigma 13440), 8.5 ml water and 1 ml 10 N NaOH. Add immediately to the pelleted worms, vortex/mix 5 s and let stand for 2 min. Repeat 3  $\times$ . Check if all worms are dissolved under the dissecting scope (only embryos are visible).
5. Pellet embryos (1000 g, 2 min), aspirate supernatant, resuspend in M9.
6. Repeat wash step with M9 4  $\times$ .
7. After the last wash, resuspend embryos in  $n \times 10$   $\mu$ l M9 ( $n$  = number of slides to prepare).
8. Get dry ice, put a metal block on dry ice for better cold conduction.
9. Add  $n \times 10$   $\mu$ l 4% PAF in water. Once PAF solution is added, start timer (5 min).
10. Distribute 20  $\mu$ l per slide, cover with 20  $\times$  20 mm coverslip.
11. After 5 min: transfer slides to the metal block on dry ice.
12. Keep slides with embryos at  $-80$  °C in a closed box or sealed plastic bag until use (to avoid desiccation).



**FIGURE 13.3**

Detection of individual NPCs by super-resolution structured illumination microscopy (SR-SIM). (A) Maximum projection of SR-SIM images of a wild-type worm embryo immunostained with anti-LMN-1 (lamin) rabbit antiserum (red) and with a pan-FG repeat nucleoporins antibody (Mab414, green). (B–D) Higher magnification of a mid-section of a nucleus. Individual pores are visible. Bars, 5  $\mu\text{m}$  in upper image and 1  $\mu\text{m}$  in lower images.

(A) Image modified from Rohner et al. (2013).

### IMMUNOFLUORESCENCE

1. Crack open eggshells by removing coverslip rapidly with a scalpel blade.
2. Transfer slide immediately to  $-20\text{ }^{\circ}\text{C}$  ethanol for dehydration for exactly 2 min.
3. Remove slides from ethanol, let air dry until no ethanol droplets are visible.
4. To save antibody solution and ensure that the embryos will not dry, we recommend using a hydrophobic delimiting pen (DAKO S2002) to trace the zone around the embryos and limit the spread of the solution.
5. Wash  $3 \times 5$  min in PBS 0.25% Triton X-100.
6. Block with 150  $\mu\text{l}$  PBS 0.25% Triton X-100 0.5% BSA for 30 min at room temperature.

7. Add 150  $\mu$ l primary antibody solution per slide in PBS 0.25% Triton X-100 0.5% BSA for 1 h at room temperature.
8. Wash  $3 \times 5$  min in PBS 0.25% Triton X-100.
9. Readd hydrophobic pen.
10. Add 150  $\mu$ l secondary antibody solution in PBS 0.25% X-100 0.5% BSA for 1 h at room temperature. The choice of fluorophores for secondary antibodies depends on the laser lines of the acquisition device.
11. Counterstain 5 min in Hoechst 33258 (4  $\mu$ l 1 mg/ml stock solution in 70 ml PBS 0.25% Triton X-100).
12. Wash  $3 \times 5$  min in PBS 0.25% Triton X-100.
13. Mount by adding a drop of ProLong antifade (Invitrogen P9634) and place a coverslip on top.
14. Fix coverslip corners with nailpolish or VALAP.
15. Cure overnight.
16. Seal completely with nailpolish or VALAP.

## IMAGING

Slides can be imaged by classical epifluorescence microscopy, laser scanning microscopy, spinning disk confocal microscopy, or advanced super-resolution microscopy. For the latter (Fig. 13.3), we used a super-resolution structured illumination microscope (Elyra S.1 [Carl Zeiss], Plan-Apochromat  $63 \times / 1.4$  NA objective lens, EM-CCD camera [iXon 885; Andor Technology], and ZEN Blue 2010 D software [Carl Zeiss]). Processing was performed with Zen software (Carl Zeiss) and 3D reconstruction and analysis were performed with Imaris software.

## MATERIALS

Antibodies and recommended dilutions

Primary antibodies used for the example in Fig. 13.3 (see also Table 13.5):

anti-NPC (pan-FG), MAb414 (mouse, ab24609, Abcam) 1/300

anti-lamin (LMN-1, rabbit, Y. Gruenbaum laboratory) 1/1000

Secondary antibodies (all 1/2000, optimized for Zeiss Elyra with laser lines at 488, 561, and 642 nm):

Alexa Fluor 488 chicken antirat (Invitrogen A-21470)

Alexa Fluor 488 goat antirabbit (Invitrogen A-11039)

Alexa Fluor 647 donkey antirabbit (Invitrogen A-31573)

Alexa Fluor 555 goat antimouse (Invitrogen A-21422)

Paraformaldehyde (PAF) 4% in  $\text{NaPO}_4$  buffer.

PAF can be prepared in advance from powder, 2 g are dissolved in 42 ml 0.1 M  $\text{Na}_2\text{HPO}_4$  with moderate heating. Once dissolved, 0.1 M  $\text{NaH}_2\text{PO}_4$  is added to 50 ml and aliquots are stored at  $-20^\circ\text{C}$ . Thawed PAF aliquots should not be refrozen.

### 13.5.2 Transmission electron microscopy

Transmission electron microscopy (TEM) has provided tremendous insight into *C. elegans* anatomy and has been instrumental to elucidate the complete wiring diagram of its nervous system (see <http://www.wormatlas.org> and <http://wormwiring.org>). TEM analyses of germline and embryonic nuclei have also contributed to the understanding of NPC structure and interaction with perinuclear P granules (e.g., Franz et al., 2005; Sheth et al., 2010; Fig. 13.4). Samples can be prepared by high-pressure freezing/freeze substitution (Franz et al., 2005; see protocol below); or chemical fixation (Sheth et al., 2010). The uterus of gravid hermaphrodites typically contains two rows of developmentally arranged embryos from zygotes distally to 50- to 100-cell stage embryos proximally, which ease identification of comparable embryos.

1. Transfer hermaphrodites to planchettes filled with 20% BSA and cryoimmobilize immediately (e.g., in a Leica EMPact high-pressure freezer).
2. Freeze-substitute samples for 48 h at  $-80^{\circ}\text{C}$  in acetone containing 2% osmium tetroxide 0.1% uranyl acetate and 5% water.

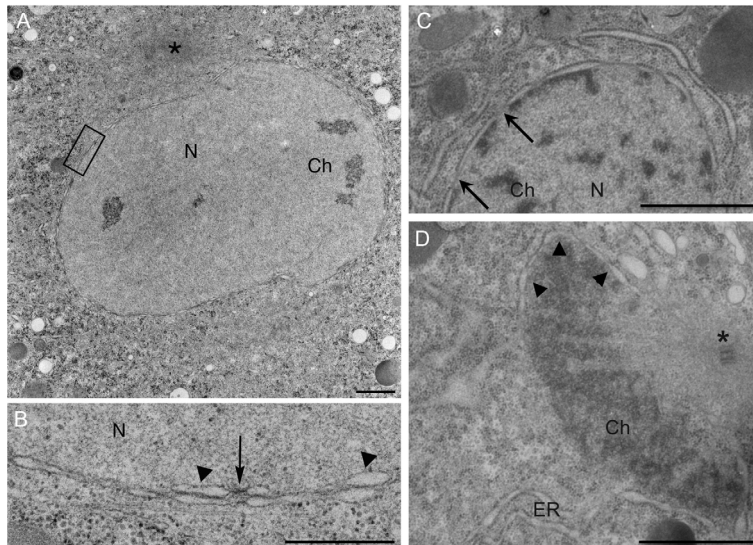


**FIGURE 13.4**

*C. elegans* NE and NPCs display classical morphology and dynamics by transmission electron microscopy. Overview (A) and a detailed view (B) of the NE in a prometaphase cell of an early embryo fixed by high-pressure freezing *in utero*. Interphase NE (C) and reforming telophase NE (D) associated with chromatin are shown. Stacked NE (arrowheads in B) is seen at prometaphase with aligned NPCs (arrow in B). Endoplasmic reticulum (ER), nucleus (N), Nuclear pore complexes (arrows), NE (arrow heads), centrosomes (\*), and chromatin (Ch) are indicated. Bars, 2  $\mu\text{m}$  (A), 500 nm (B), and 1  $\mu\text{m}$  (C and D).

*Adapted from Galy et al. (2008).*

3. Warm samples to  $-30^{\circ}\text{C}$  for 3 h and then gradually to room temperature ( $5^{\circ}\text{C/h}$ ).
4. After several acetone rinses, infiltrate samples with Epon resin during 48 h.
5. Flat embed samples in a thin layer of resin and polymerize at  $60^{\circ}\text{C}$  during 48 h.
6. Mount thin sections on standard microscope slides and select the worms and embryos of interest.
7. Mount ultrathin sections on Formvar-coated copper grids and stain with 2% uranyl acetate in water and lead citrate.
8. Image grids with a transmission electron microscope (e.g., a 10-kV Jeol JEM-1010 electron microscope).

---

### 13.6 INTERACTION OF NUPS WITH CHROMATIN

Numerous recent studies have demonstrated that nups play an active role interacting with chromatin, not only at NPCs but also in the nucleoplasm (reviewed in [Liang & Hetzer, 2011](#)). Such interactions have been described in several organisms, including yeast, flies, and humans but have only begun to be explored in nematodes recently. Interactions between nups and chromatin can be assessed by chromatin immunoprecipitation (ChIP), Dam-mediated methylation (DamID), and super-resolution microscopy.

Super-resolution microscopy (see [Section 13.1.5](#)) can be used to precisely determine where a given sequence of the genome is localized in relation to perinuclear compartments. The sequence of interest is labeled by integrating lacO repeats in its proximity while expressing the lacI repressor fused to a fluorescent protein, for example, GFP. This leads to the local accumulation of GFP-lacI on the lacO repeats and the formation of a readily detectable spot inside the nucleus ([Meister, Towbin, Pike, Ponti, & Gasser, 2010](#)). Super-resolution microscopy of the nuclear lamina and NPCs combined with the lacO/lacI technique was notably used to demonstrate colocalization of the heat-shock induced promoter *hsp-16.2* with NPCs in embryos ([Rohner et al., 2013](#)).

Immunoprecipitation of nups is challenging, as proteins are poorly soluble and heavily crosslinked together during the chromatin cross-linking process. Nevertheless, ChIP has been carried out with antibodies for three pore-related proteins by the laboratory of Jason Lieb: two nups, NPP-13 (NUP93) and NPP-3 (NUP205) as well as the pore-associated importin IMB-1 (KPNB1/importin  $\beta$ 1). Interestingly, all three proteins interact with PolIII-transcribed noncoding RNA genes, either transfer RNAs (tRNAs) or small nucleolar RNAs (snoRNAs) ([Ikegami & Lieb, 2013](#)). This study further indicated that these ncRNAs genes are located very close to or even inside the nuclear pore lumen and that the interaction of pore proteins with ncRNAs coordinates transcription and processing ([Ikegami & Lieb, 2013](#)).

As an alternative to ChIP, interactions between chromatin and NPC-related proteins may be studied by fusing the latter with *E. coli* Dam methyltransferase, a method known as DamID. Expression of the fusion proteins generates *in vivo* interaction

maps that can be analyzed on microarrays or by direct sequencing. In particular, DamID may be an attractive method if specific antibodies are not available and has provided valuable insight into anchoring of heterochromatin to the nuclear lamina (Towbin et al., 2012). However, no NPC-related dataset has been published to date using this technique. Detailed protocols for ChIP and DamID in *C. elegans* are available on WormBook (Askjaer, Ercan, & Meister, 2014).

## SUMMARY AND FUTURE PERSPECTIVES

Studies of *C. elegans* NPC structure and function has so far mainly focused on early embryos. However, based on experience from other organisms (Gomez-Cavazos & Hetzer, 2012), it is conceivable that also nematode nups and transport factors are expressed and function in tissue-specific manners. Most fluorescent markers have been constructed with heterologous promoters to favor expression in early embryos because of their suitability for live imaging. Analysis of mRNA levels suggests that relative expression levels among nups differ significantly during the lifespan of the animal (D'Angelo et al., 2009), but information on protein concentration within and across tissues is still scarce. Generation of strains that stably express tagged nups from single-copy transgenes containing their own promoter or by CRISPR-Cas9-mediated GFP knock-in into endogenous loci is an ongoing effort that is likely to yield exciting observations.

Large-scale RNAi screens have revealed unexpected roles of *C. elegans* nups in diverse processes, such as regulation of mitotic spindle position, tumor growth, P granule dynamics, transposon silencing, RNAi efficiency, and protection against DNA damage (Table 13.1). Because most of these studies were designed to retrieve candidate genes rather than uncover molecular mechanisms many open questions remain: Can these phenotypes (partially) be explained by altered nucleocytoplasmic transport or do they reflect truly novel functions? How specific are the phenotypes to the individual nups (i.e., are the nups that did not show up in a particular screen irrelevant for this phenotype or were their knockdowns incomplete)? Are the phenotypes manifestations of requirements for given nups in a particular tissue or during a specific developmental process? The fact that nonoverlapping sets of nups were discovered in the different screens argues against the trivial explanation of general defects in transport through the NPCs. Instead, these observations are attractive starting points for future studies. Generation of targeted mutations, now achievable via CRISPR-Cas9 technology, may help to uncover multiple functions of nucleoporins.

---

## Acknowledgments

Our laboratories are supported by the Spanish Ministry of Economy and Competitiveness (BFU2010-15478 to P. A.), the Autonomous Government of Andalusia (P08-CVI-3920 to P. A.), the European Regional Development Fund (to P. A.), the Centre National de la

Recherche Scientifique (ATIP Grant to V. G.), the University of Pierre and Marie Curie (to V. G.), the Agence Nationale de la Recherche (ANR 07-BLAN-0063-21 and ANR 12-BSV2-0018-01 to V. G.), the Association pour la Recherche contre le Cancer (to V. G.), the Bettencourt-Schueller foundation (Coup d'élan pour la recherche 2012 to V. G.), the Swiss National Foundation (SNF assistant professor grant PP00P3\_133744 to P. M.), and the University of Bern (to P. M.).

---

## References

- Askjaer, P., Ercan, S., & Meister, P. (2014). Modern techniques for the analysis of chromatin and nuclear organization in *C. elegans*. In The *C. elegans* Research Community (Ed.), *WormBook*. WormBook. <http://dx.doi.org/10.1895/wormbook.1.169.1>, <http://www.wormbook.org>.
- Askjaer, P., Galy, V., Hannak, E., & Mattaj, I. W. (2002). Ran GTPase cycle and importins alpha and beta are essential for spindle formation and nuclear envelope assembly in living *Caenorhabditis elegans* embryos. *Molecular Biology of the Cell*, *13*, 4355–4370.
- Audhya, A., Desai, A., & Oegema, K. (2007). A role for Rab5 in structuring the endoplasmic reticulum. *The Journal of Cell Biology*, *178*, 43–56.
- Bamba, C., Bobiniec, Y., Fukuda, M., & Nishida, E. (2002). The GTPase Ran regulates chromosome positioning and nuclear envelope assembly in vivo. *Current Biology*, *12*, 503–507.
- Berkowitz, L. A., Knight, A. L., Caldwell, G. A., & Caldwell, K. A. (2008). Generation of stable transgenic *C. elegans* using microinjection. *Journal of Visualized Experiments*, *18*, e833.
- Brauchle, M., Baumer, K., & Gonczy, P. (2003). Differential activation of the DNA replication checkpoint contributes to asynchrony of cell division in *C. elegans* embryos. *Current Biology*, *13*, 819–827.
- Brenner, S. (1974). The genetics of *Caenorhabditis elegans*. *Genetics*, *77*, 71–94.
- Burt, E. C., Towers, P. R., & Sattelle, D. B. (2006). *Caenorhabditis elegans* in the study of SMN-interacting proteins: A role for SMI-1, an orthologue of human Gemin2 and the identification of novel components of the SMN complex. *Invertebrate Neuroscience*, *6*, 145–159.
- Bussing, I., Yang, J. S., Lai, E. C., & Grosshans, H. (2010). The nuclear export receptor XPO-1 supports primary miRNA processing in *C. elegans* and *Drosophila*. *The EMBO Journal*, *29*, 1830–1839.
- Carvalho, A., et al. (2011). Acute drug treatment in the early *C. elegans* embryo. *PLoS ONE*, *6*, e24656.
- Chen, C., Fenk, L. A., & de Bono, M. (2013). Efficient genome editing in *Caenorhabditis elegans* by CRISPR-targeted homologous recombination. *Nucleic Acids Research*, *41*, e193.
- Cheng, H., Govindan, J. A., & Greenstein, D. (2008). Regulated trafficking of the MSP/Eph receptor during oocyte meiotic maturation in *C. elegans*. *Current Biology*, *18*, 705–714.
- Chiu, H., Schwartz, H. T., Antoshechkin, I., & Sternberg, P. W. (2013). Transgene-free genome editing in *Caenorhabditis elegans* using CRISPR-Cas. *Genetics*, *195*, 1167–1171.
- Cipriani, P. G., & Piano, F. (2011). RNAi methods and screening: RNAi based high-throughput genetic interaction screening. *Methods in Cell Biology*, *106*, 89–111.

- Cohen, M., Feinstein, N., Wilson, K. L., & Gruenbaum, Y. (2003). Nuclear pore protein gp210 is essential for viability in HeLa cells and *Caenorhabditis elegans*. *Molecular Biology of the Cell*, *14*, 4230–4237.
- D'Angelo, M. A., Raices, M., Panowski, S. H., & Hetzer, M. W. (2009). Age-dependent deterioration of nuclear pore complexes causes a loss of nuclear integrity in postmitotic cells. *Cell*, *136*, 284–295.
- Dickinson, D. J., Ward, J. D., Reiner, D. J., & Goldstein, B. (2013). Engineering the *Caenorhabditis elegans* genome using Cas9-triggered homologous recombination. *Nature Methods*, *10*, 1028–1034.
- Doitsidou, M., Poole, R. J., Sarin, S., Bigelow, H., & Hobert, O. (2010). *C. elegans* mutant identification with a one-step whole-genome-sequencing and SNP mapping strategy. *PLoS ONE*, *5*, e15435.
- Fernandez, A. G., & Piano, F. (2006). MEL-28 is downstream of the Ran cycle and is required for nuclear-envelope function and chromatin maintenance. *Current Biology*, *16*, 1757–1763.
- Fire, A., Xu, S., Montgomery, M. K., Kostas, S. A., Driver, S. E., & Mello, C. C. (1998). Potent and specific genetic interference by double-stranded RNA in *Caenorhabditis elegans*. *Nature*, *391*, 806–811.
- Franz, C., et al. (2005). Nup155 regulates nuclear envelope and nuclear pore complex formation in nematodes and vertebrates. *The EMBO Journal*, *24*, 3519–3531.
- Friedland, A. E., Tzur, Y. B., Esvelt, K. M., Colaiacovo, M. P., Church, G. M., & Calarco, J. A. (2013). Heritable genome editing in *C. elegans* via a CRISPR-Cas9 system. *Nature Methods*, *10*, 741–743.
- Frokjaer-Jensen, C., Davis, M. W., Ailion, M., & Jorgensen, E. M. (2012). Improved Mos1-mediated transgenesis in *C. elegans*. *Nature Methods*, *9*, 117–118.
- Frokjaer-Jensen, C., et al. (2008). Single-copy insertion of transgenes in *Caenorhabditis elegans*. *Nature Genetics*, *40*, 1375–1383.
- Galy, V., Askjaer, P., Franz, C., Lopez-Iglesias, C., & Mattaj, I. W. (2006). MEL-28, a novel nuclear-envelope and kinetochore protein essential for zygotic nuclear-envelope assembly in *C. elegans*. *Current Biology*, *16*, 1748–1756.
- Galy, V., Mattaj, I. W., & Askjaer, P. (2003). *Caenorhabditis elegans* nucleoporins Nup93 and Nup205 determine the limit of nuclear pore complex size exclusion *in vivo*. *Molecular Biology of the Cell*, *14*, 5104–5115.
- Galy, V., et al. (2008). A role for gp210 in mitotic nuclear-envelope breakdown. *Journal of Cell Science*, *121*, 317–328.
- Geles, K. G., & Adam, S. A. (2001). Germline and developmental roles of the nuclear transport factor importin alpha3 in *C. elegans*. *Development*, *128*, 1817–1830.
- Geles, K. G., Johnson, J. J., Jong, S., & Adam, S. A. (2002). A role for *Caenorhabditis elegans* importin IMA-2 in germ line and embryonic mitosis. *Molecular Biology of the Cell*, *13*, 3138–3147.
- Gomez-Cavazos, J. S., & Hetzer, M. W. (2012). Outfits for different occasions: Tissue-specific roles of nuclear envelope proteins. *Current Opinion in Cell Biology*, *24*, 775–783.
- Gonczy, P. (2008). Mechanisms of asymmetric cell division: Flies and worms pave the way. *Nature Reviews. Molecular Cell Biology*, *9*, 355–366.
- Gonczy, P., et al. (2001). *zyg-8*, a gene required for spindle positioning in *C. elegans*, encodes a doublecortin-related kinase that promotes microtubule assembly. *Developmental Cell*, *1*, 363–375.

- Gorjanacz, M., et al. (2007). *Caenorhabditis elegans* BAF-1 and its kinase VRK-1 participate directly in post-mitotic nuclear envelope assembly. *The EMBO Journal*, *26*, 132–143.
- Grill, B., et al. (2012). RAE-1, a novel PHR binding protein, is required for axon termination and synapse formation in *Caenorhabditis elegans*. *The Journal of Neuroscience*, *32*, 2628–2636.
- Gruenbaum, Y., Lee, K. K., Liu, J., Cohen, M., & Wilson, K. L. (2002). The expression, lamin-dependent localization and RNAi depletion phenotype for emerlin in *C. elegans*. *Journal of Cell Science*, *115*, 923–929.
- Gupta, B. P., & Sternberg, P. W. (2002). Tissue-specific regulation of the LIM homeobox gene *lin-11* during development of the *Caenorhabditis elegans* egg-laying system. *Developmental Biology*, *247*, 102–115.
- Hachet, V., Busso, C., Toya, M., Sugimoto, A., Askjaer, P., & Gonczy, P. (2012). The nucleoporin Nup205/NPP-3 is lost near centrosomes at mitotic onset and can modulate the timing of this process in *Caenorhabditis elegans* embryos. *Molecular Biology of the Cell*, *23*, 3111–3121.
- Hadwiger, G., Dour, S., Arur, S., Fox, P., & Nonet, M. L. (2010). A monoclonal antibody toolkit for *C. elegans*. *PLoS ONE*, *5*, e10161.
- Hajeri, V. A., Little, B. A., Ladage, M. L., & Padilla, P. A. (2010). NPP-16/Nup50 function and CDK-1 inactivation are associated with anoxia-induced prophase arrest in *Caenorhabditis elegans*. *Molecular Biology of the Cell*, *21*, 712–724.
- Hochbaum, D., Ferguson, A. A., & Fisher, A. L. (2010). Generation of transgenic *C. elegans* by biolistic transformation. *Journal of Visualized Experiments*, *42*, e2090.
- Ikegami, K., Egelhofer, T. A., Strome, S., & Lieb, J. D. (2010). *Caenorhabditis elegans* chromosome arms are anchored to the nuclear membrane via discontinuous association with LEM-2. *Genome Biology*, *11*, R120. <http://dx.doi.org/10.1186/gb-2010-11-12-r120>.
- Ikegami, K., & Lieb, J. D. (2013). Integral nuclear pore proteins bind to Pol III-transcribed genes and are required for Pol III transcript processing in *C. elegans*. *Molecular Cell*, *51*, 540–549. <http://dx.doi.org/10.1016/j.molcel.2013.08.001>.
- Kamath, R. S., & Ahringer, J. (2003). Genome-wide RNAi screening in *Caenorhabditis elegans*. *Methods*, *30*, 313–321.
- Katic, I., & Grosshans, H. (2013). Targeted heritable mutation and gene conversion by Cas9-CRISPR in *Caenorhabditis elegans*. *Genetics*, *195*, 1173–1176.
- Kim, S., & Yu, H. (2011). Mutual regulation between the spindle checkpoint and APC/C. *Seminars in Cell and Developmental Biology*, *22*, 551–558.
- Kim, J. K., et al. (2005). Functional genomic analysis of RNA interference in *C. elegans*. *Science*, *308*, 1164–1167.
- Kostic, I., & Roy, R. (2002). Organ-specific cell division abnormalities caused by mutation in a general cell cycle regulator in *C. elegans*. *Development*, *129*, 2155–2165.
- Kuersten, S., Segal, S. P., Verheyden, J., LaMartina, S. M., & Goodwin, E. B. (2004). NXF-2, REF-1, and REF-2 affect the choice of nuclear export pathway for *tra-2* mRNA in *C. elegans*. *Molecular Cell*, *14*, 599–610.
- Lee, K. K., Gruenbaum, Y., Spann, P., Liu, J., & Wilson, K. L. (2000). *C. elegans* nuclear envelope proteins emerlin, MAN1, lamin, and nucleoporins reveal unique timing of nuclear envelope breakdown during mitosis. *Molecular Biology of the Cell*, *11*, 3089–3099.
- Liang, Y., & Hetzer, M. W. (2011). Functional interactions between nucleoporins and chromatin. *Current Opinion in Cell Biology*, *23*, 65–70.



- Lo, T. W., et al. (2013). Precise and heritable genome editing in evolutionarily diverse nematodes using TALENs and CRISPR/Cas9 to engineer insertions and deletions. *Genetics*, *195*, 331–348.
- McNally, F. J. (2013). Mechanisms of spindle positioning. *The Journal of Cell Biology*, *200*, 131–140.
- Meister, P., Towbin, B. D., Pike, B. L., Ponti, A., & Gasser, S. M. (2010). The spatial dynamics of tissue-specific promoters during *C. elegans* development. *Genes & Development*, *24*, 766–782.
- Merritt, C., Gallo, C. M., Rasoloson, D., & Seydoux, G. (2010). Transgenic solutions for the germline. In The *C. elegans* Research Community (Ed.), *WormBook*. WormBook. <http://dx.doi.org/10.1895/wormbook.1.148.1>, <http://www.wormbook.org>.
- Nakamura, K., et al. (2005). Wnt signaling drives WRM-1/beta-catenin asymmetries in early *C. elegans* embryos. *Genes & Development*, *19*, 1749–1754.
- Olson, S. K., Greenan, G., Desai, A., Muller-Reichert, T., & Oegema, K. (2012). Hierarchical assembly of the eggshell and permeability barrier in *C. elegans*. *The Journal of Cell Biology*, *198*, 731–748.
- O'Rourke, S. M., Dorfman, M. D., Carter, J. C., & Bowerman, B. (2007). Dynein modifiers in *C. elegans*: Light chains suppress conditional heavy chain mutants. *PLoS Genetics*, *3*, e128.
- Pinkston-Gosse, J., & Kenyon, C. (2007). DAF-16/FOXO targets genes that regulate tumor growth in *Caenorhabditis elegans*. *Nature Genetics*, *39*, 1403–1409.
- Praitis, V. (2006). Creation of transgenic lines using microparticle bombardment methods. *Methods in Molecular Biology*, *351*, 93–107.
- Pushpa, K., Kumar, G. A., & Subramaniam, K. (2013). PUF-8 and TCER-1 are essential for normal levels of multiple mRNAs in the *C. elegans* germline. *Development*, *140*, 1312–1320.
- Putker, M., et al. (2013). Redox-dependent control of FOXO/DAF-16 by transportin-1. *Molecular Cell*, *49*, 730–742.
- Querido, E., & Chartrand, P. (2008). Using fluorescent proteins to study mRNA trafficking in living cells. *Methods in Cell Biology*, *85*, 273–292.
- Raj, A., van den Bogaard, P., Rifkin, S. A., van Oudenaarden, A., & Tyagi, S. (2008). Imaging individual mRNA molecules using multiple singly labeled probes. *Nature Methods*, *5*, 877–879.
- Reese, K. J., Dunn, M. A., Waddle, J. A., & Seydoux, G. (2000). Asymmetric segregation of PIE-1 in *C. elegans* is mediated by two complementary mechanisms that act through separate PIE-1 protein domains. *Molecular Cell*, *6*, 445–455.
- Robert, V. J., & Bessereau, J. L. (2011). Genome engineering by transgene-instructed gene conversion in *C. elegans*. *Methods in Cell Biology*, *106*, 65–88.
- Robert, V. J., Sijen, T., van Wolfswinkel, J., & Plasterk, R. H. (2005). Chromatin and RNAi factors protect the *C. elegans* germline against repetitive sequences. *Genes & Development*, *19*, 782–787.
- Rodenas, E., Gonzalez-Aguilera, C., Ayuso, C., & Askjaer, P. (2012). Dissection of the NUP107 nuclear pore subcomplex reveals a novel interaction with spindle assembly checkpoint protein MAD1 in *Caenorhabditis elegans*. *Molecular Biology of the Cell*, *23*, 930–944.
- Rodenas, E., Klerkx, E. P., Ayuso, C., Audhya, A., & Askjaer, P. (2009). Early embryonic requirement for nucleoporin Nup35/NPP-19 in nuclear assembly. *Developmental Biology*, *327*, 399–409.

- Rohner, S., et al. (2013). Promoter- and RNA polymerase II-dependent *hsp-16* gene association with nuclear pores in *Caenorhabditis elegans*. *The Journal of Cell Biology*, *200*, 589–604.
- Rual, J. F., et al. (2004). Toward improving *Caenorhabditis elegans* phenome mapping with an ORFeome-based RNAi library. *Genome Research*, *14*, 2162–2168.
- Schetter, A., Askjaer, P., Piano, F., Mattaj, I., & Kemphues, K. (2006). Nucleoporins NPP-1, NPP-3, NPP-4, NPP-11 and NPP-13 are required for proper spindle orientation in *C. elegans*. *Developmental Biology*, *289*, 360–371.
- Shakes, D. C., Miller, D. M., 3rd., & Nonet, M. L. (2012). Immunofluorescence microscopy. *Methods in Cell Biology*, *107*, 35–66.
- Sheth, U., Pitt, J., Dennis, S., & Priess, J. R. (2010). Perinuclear P granules are the principal sites of mRNA export in adult *C. elegans* germ cells. *Development*, *137*, 1305–1314.
- Simpson, K. J., Davis, G. M., & Boag, P. R. (2012). Comparative high-throughput RNAi screening methodologies in *C. elegans* and mammalian cells. *New Biotechnology*, *29*, 459–470.
- Sonnichsen, B., et al. (2005). Full-genome RNAi profiling of early embryogenesis in *Caenorhabditis elegans*. *Nature*, *434*, 462–469.
- Stavru, F., Hulsmann, B. B., Spang, A., Hartmann, E., Cordes, V. C., & Gorlich, D. (2006). NDC1: A crucial membrane-integral nucleoporin of metazoan nuclear pore complexes. *The Journal of Cell Biology*, *173*, 509–519.
- Strome, S., et al. (2001). Spindle dynamics and the role of gamma-tubulin in early *Caenorhabditis elegans* embryos. *Molecular Biology of the Cell*, *12*, 1751–1764.
- Sulston, J. E., & Horvitz, H. R. (1977). Post-embryonic cell lineages of the nematode, *Caenorhabditis elegans*. *Developmental Biology*, *56*, 110–156.
- Sulston, J. E., Schierenberg, E., White, J. G., & Thomson, J. N. (1983). The embryonic cell lineage of the nematode *Caenorhabditis elegans*. *Developmental Biology*, *100*, 64–119.
- Takeda, K., Watanabe, C., Qadota, H., Hanazawa, M., & Sugimoto, A. (2008). Efficient production of monoclonal antibodies recognizing specific structures in *Caenorhabditis elegans* embryos using an antigen subtraction method. *Genes to Cells*, *13*, 653–665.
- Tinevez, J. Y., et al. (2012). A quantitative method for measuring phototoxicity of a live cell imaging microscope. *Methods in Enzymology*, *506*, 291–309.
- Towbin, B. D., et al. (2012). Step-Wise Methylation of Histone H3K9 Positions Heterochromatin at the Nuclear Periphery. *Cell*, *150*, 934–947.
- Tzur, Y. B., Friedland, A. E., Nadarajan, S., Church, G. M., Calarco, J. A., & Colaiacovo, M. P. (2013). Heritable custom genomic modifications in *caenorhabditis elegans* via a CRISPR-Cas9 system. *Genetics*, *195*, 1181–1185.
- Urdike, D. L., Hachey, S. J., Kreher, J., & Strome, S. (2011). P granules extend the nuclear pore complex environment in the *C. elegans* germ line. *The Journal of Cell Biology*, *192*, 939–948.
- Urdike, D. L., & Strome, S. (2009). A genomewide RNAi screen for genes that affect the stability, distribution and function of P granules in *Caenorhabditis elegans*. *Genetics*, *183*, 1397–1419.
- Vallin, E., et al. (2012). A genome-wide collection of Mos1 transposon insertion mutants for the *C. elegans* research community. *PLoS ONE*, *7*, e30482.
- van Haften, G., et al. (2006). Identification of conserved pathways of DNA-damage response and radiation protection by genome-wide RNAi. *Current Biology*, *16*, 1344–1350.
- Vastenhouw, N. L., et al. (2003). A genome-wide screen identifies 27 genes involved in transposon silencing in *C. elegans*. *Current Biology*, *13*, 1311–1316.

- Voronina, E., & Seydoux, G. (2010). The *C. elegans* homolog of nucleoporin Nup98 is required for the integrity and function of germline P granules. *Development*, *137*, 1441–1450.
- Waijers, S., et al. (2013). CRISPR/Cas9-targeted mutagenesis in *Caenorhabditis elegans*. *Genetics*, *195*, 1187–1191.
- Walther, T. C., et al. (2003). RanGTP mediates nuclear pore complex assembly. *Nature*, *424*, 689–694.
- Wong, I., White, S., Buchner, M., Srayko, M., & Muller-Reichert, T. (2012). Correlative light and electron microscopy of intermediate stages of meiotic spindle assembly in the early *Caenorhabditis elegans* embryo. *Methods in Cell Biology*, *111*, 223–234.
- Zeiser, E., Frokjaer-Jensen, C., Jorgensen, E., & Ahringer, J. (2011). MosSCI and gateway compatible plasmid toolkit for constitutive and inducible expression of transgenes in the *C. elegans* germline. *PLoS ONE*, *6*, e20082.
- Zuryn, S., Le Gras, S., Jamet, K., & Jarriault, S. (2010). A strategy for direct mapping and identification of mutations by whole-genome sequencing. *Genetics*, *186*, 427–430.